ORIGINAL RESEARCH Open access

Design of a Gripper Prototype for UAV-Based Manipulation of Helical Bird Diverters

Amira Khalil[1*], Sara Fathy[1], Mahmoud Adel[2], Hany Nabil[3], Rania Mostafa[4]

Abstract

Power grids form an essential foundation for every nation's infrastructure. These networks include extensive lengths of power lines that demand routine checks and servicing. Important activities include placing and removing bird diverters to reduce the risk of birds hitting the lines. Such devices help birds notice cables more easily and reduce the risk of collisions. Usually, people perform these installation and removal tasks from helicopters or directly on the lines. Beyond the substantial costs, working at great heights poses serious risks to human safety. To address these hazards, this paper proposes an original method for automating the procedures. The suggested approach features a prototype gripper meant to attach to unmanned aerial vehicles (UAVs) and be controlled remotely for installing or detaching bird diverters. This research details the mechatronic tool and its software framework, which were tested in a lab setup. The setup used a robotic arm fitted with the new tool to detach a bird diverter. Additional effort will be required to mount the suggested tool on a UAV.

Keywords Inspection and maintenance, Power lines, Aerial manipulators, UAV-based crop monitoring

*Correspondence:
Amira Khalil
amira.khalil@alexu.edu.eg
[1] Department of AI for Fennel and Anise Essential Oil Yield Optimization, Faculty of Agriculture, Alexandria University, Alexandria, Egypt
[2] Department of Smart Harvest Time Prediction, Faculty of Agriculture, Cairo University, Cairo, Egypt
[3] Department of Machine Learning for Oil Quality Grading, Faculty of Agriculture, Mansoura University, Mansoura, Egypt
[4] Department of Precision Drying Temperature Control, Faculty of Agriculture, Helwan University, Cairo, Egypt

Introduction

Above-ground electricity transmission and distribution lines are growing due to population growth and higher energy demand. These lines pose major threats to many bird species, disrupting their breeding, nesting, and wintering areas [1]. Bird deaths from power lines reach notable levels in areas with abundant birdlife, particularly among species with unique behaviors (e.g., eagle owls) or during conditions that facilitate migrant movement. Such incidents are thought to involve roughly 350 bird species [2]. In contrast, yearly bird deaths from power lines total 1 million in the Netherlands, 175 million in the United States [3], and nearly 1 billion worldwide [4]. In addition to killing birds, impacts with power lines pose problems for utility firms by potentially triggering blackouts after collisions [5]. Because of this, several tools called bird diverters were developed to increase the visibility of power lines to birds and prevent them from getting too close.

A wide variety of bird diverters exists for purchase. Typical ones appear in **Figure 1**, such as the clip-type diverter (left) and the helical bird diverter (right). These tools fall mostly into active **(Figure 1 (left))** and passive **(Figure 1 (right))** groups. Active versions contain a moving section driven by wind. Passive types often include helical shapes made from plastic or aluminium components that coil around the power cable **(Figure 1)**.

This is an open access article distributed under the terms of the Creative Commons Attribution-NonCommercial-ShareAlike 4.0 International License (CC BY-NC-SA 4.0), which permits non-commercial use, distribution, reproduction, and adaptation in any medium or format, provided that appropriate credit is given to the original author(s) and source, a link to the license is provided, and any changes made are indicated. Adapted material must be distributed under the same license.

© 2025 The Author(s). | Published by Agro Intelligence Research Press

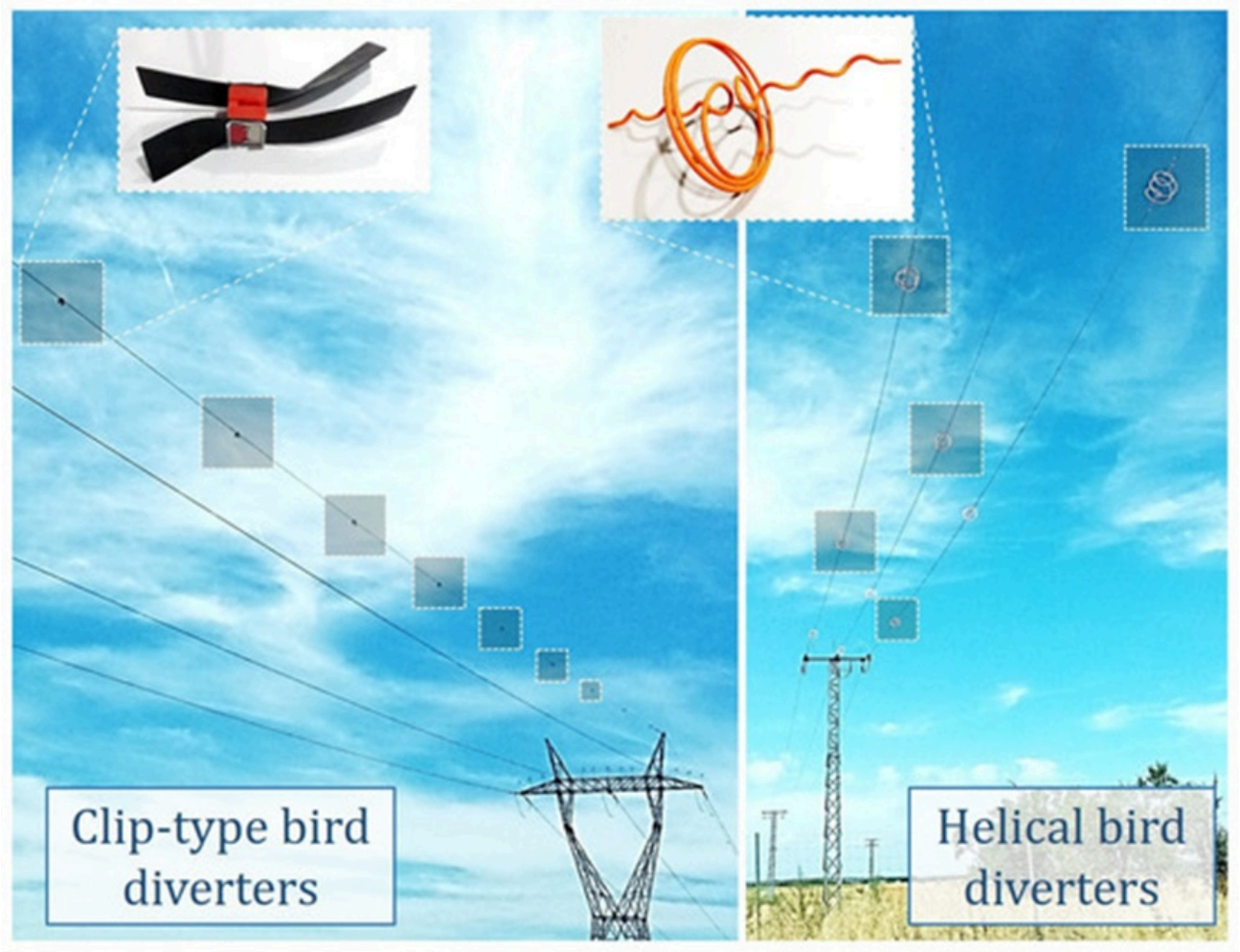

Figure 1. Different bird diverters are installed on power lines.

Installation of bird diverters normally relies on skilled human workers who access the cables via aerial lifts, helicopters, or other elevated equipment. The work tends to be expensive and risky owing to extreme heights (15–50 m). Furthermore, even with the line switched off, workers risk touching energized parts. This calls for stricter safety rules, including the use of conductive clothing or special insulated equipment, which would make the job even harder.

This study limits itself to handling helical bird diverters among the available options, given that their fitting and detachment involve particularly tricky steps. The procedure breaks down into these stages:

- Slide the wider end of the bird diverter over the conductor or strand **(Figure 2a)**.
- Turn the bird diverter so the initial helix settles properly beside the power line **(Figure 2b)**.
- Coil the fastening helix tightly around the power line **(Figure 2c)**.

© 2025 The Author(s). | Published by Agro Intelligence Research Press

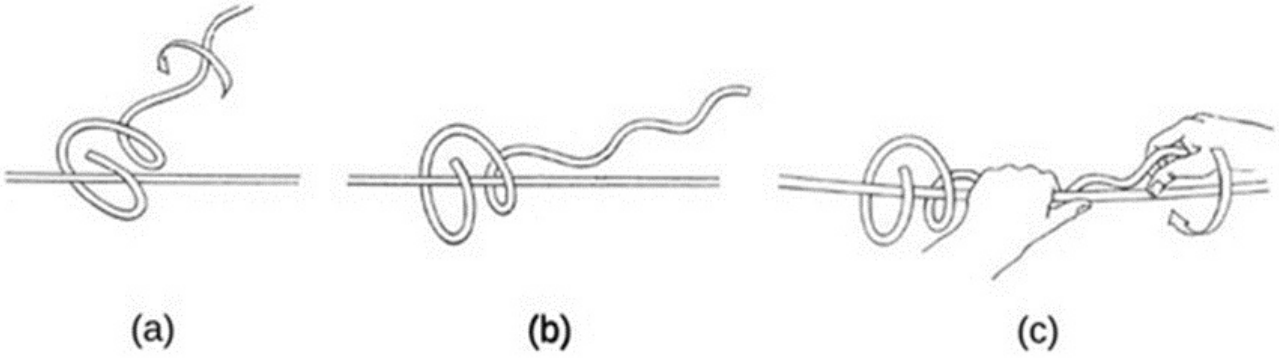

Figure 2. Installation process of the bird flight diverter, from (a) to (c), the insertion of the diverter and its rotation around the power cable to lock it.

To detach the diverter, the same steps must be performed in reverse order.

Beyond initial fitting, bird diverters also require regular maintenance and replacement over time. Taking them off brings its own set of problems. This paper proposes a novel mechatronic approach to address the detachment of helical bird diverters.

The planned system uses an autonomous unmanned aerial vehicle (UAV) that carries a custom gripper designed to remove bird diverters. A human operator flies the UAV by remote control toward the target spot, after which the vehicle can identify the helical bird diverter on the line by itself. This data then helps locate the best spot to grab it and triggers the automatic detachment sequence. Thanks to this setup, the operator remains safely on the ground to monitor the process and returns the UAV to base once the process is complete.

Core achievements of this work include the introduction of the built prototype **(Figure 3)** and the machine learning method for detecting the bird diverter's location and direction to guide the gripper's movements during removal. The results shown here were obtained under controlled lab conditions, where the gripper was mounted on a standard robotic arm and the power line network was recreated using a suitable model. Upcoming research will involve actual UAVs to progress further.

© 2025 The Author(s). | Published by Agro Intelligence Research Press



Figure 3. Bird diverter removal device.

The paper continues in this order: Section 2 reviews comparable existing systems. Section 3 explores the suggested prototype. Section 4 describes the complete system design, while Section 5 tests the solution inside a lifelike industrial setting. Lastly, Section 6 summarizes the findings and outlines the next steps.

Related Works

Bird diverters exist to raise awareness of overhead cables among birds. They sometimes use shifting colours across the three phases of a power line to boost performance **(Figure 1)** [6]. Lately, more attention has been paid to flying systems that can attach these tools. In broad terms, aerial manipulators [7] help with inspections and repairs in hard-to-reach or unsafe areas, such as oil and gas pipelines [8-10], chemical facilities, and bridges [11, 12], as well as fitting equipment, operating valves, and similar maintenance tasks [13-16]. Different carriers can handle large loads such as full industrial robotic arms [17, 18].

Focusing on power network preservation, multiple papers have examined UAV applications. One example in Ref. [19] shows a setup that perches on power lines using a LIDAR sensor. On the other hand, Ref. [20] introduces a compressed-air method for placing devices onto lines. Still, because of the spiral form of helical bird diverters, this compressed-air idea does not fit the needs of the current task.

© 2025 The Author(s). | Published by Agro Intelligence Research Press

Clip-style diverters represent another frequent variety. Earlier projects have already tried installing this style. Work in Ref. [21] applied an aerial robot for clip-type units, and Ref. [22] offered a light dual-arm platform for helical ones.

Proper removal of helical bird diverters demands a well-suited gripper design. Studies on grippers and holding methods go from basic claw styles [23] to advanced models [24, 25]. Thorough summaries of such tools appear in Refs. [26] and [27]. Even so, two arms become necessary due to the motions needed for handling helical diverters **(Figure 2)**. Among current options, the LiCAS A1 [28] stands out as a light and flexible dual-arm unit [29] offering 4 degrees of freedom on each arm. Earlier use of this system for helical diverter handling occurred in Ref. [22]. Yet our design stays simpler by avoiding complicated path calculations. Moreover, that prior study covered only the initial phases of installation and skipped more challenging handling steps, which the writers indicated might require clamp adjustments.

The biggest contrast with earlier methods lies in our system's need for just one contact point at the outer end of the helical diverter. Continuous spinning around the cable, enabled by the tool, allows for full installation or removal. We also conducted trials in a lab model using a stationary industrial arm rather than a flying one. That said, studies in Ref. [30] have already looked into similar aerial handling and human-robot teamwork for mounting bird diverters.

Lastly, camera input helps the task recognize the helical item, allowing it to run without direct control. More precisely, the YOLO (You Only Look Once) V4 method [31, 32] processed image data from an Intel RealSense depth camera. YOLO is a popular choice mainly for object detection. Here, we adjusted and trained the YOLO system to spot helical bird diverters.

Bird Diverter Manipulation Device

This section explains the mechanical structure of the tool used to handle bird diverters.

At its heart, the tool created here relies on a single spinning unit to manage the diverter and coil it onto the cable. Such a method simplifies the challenges shown in **Figure 2** for helical items. Extra Degrees of Freedom (DoFs) required to complete the job (such as forward movement along the cable) are provided by the flying platform. The gripper itself uses just one DoF.

Details of the gripper's build follow next. The prototype includes 41 common mechanical and electronic pieces. Eleven special components were created and produced via 3D printing in PET-G to maintain strength during use. Total measurements reach (255×292×80) mm, with a mass of nearly 3.1 kg.

Engineering focused on a worm gear paired with a toothed wheel for a strong turning force, even at slow rates, plus a guillotine part to lock the diverter inside the wheel. Every inner element fits within an outer frame composed of three sections: upper, lower, and rear. Each part has a round opening for the toothed wheel. A 30-degree round gap also allows the device to catch the electric cable, as shown on the left side of **Figure 4**.

© 2025 The Author(s). | Published by Agro Intelligence Research Press

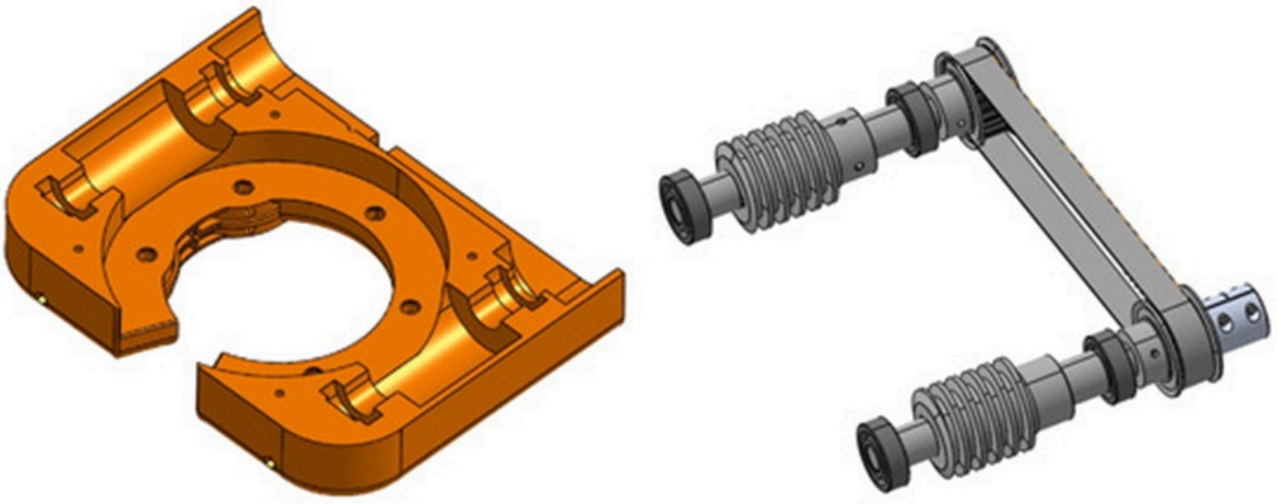

Figure 4. Left: external chassis of the device; right: system shafts.

The device's chassis interior was designed to accommodate the motor and its associated driven shafts. Assembly of this section is shown on the right side of **Figure 4**.

Each shaft in this arrangement features a central portion measuring 16 mm and two end segments measuring 12 mm each. Components that secure the worm screw against rotation and support the pulley reside on these sections. The worm screw is the first item fitted onto the shafts. Furthermore, the shafts incorporate opposing thread directions to support both right-handed and left-handed turning. Their terminal ends include spacers with 20 mm and 18 mm diameters, followed by ball bearings with a dynamic load capacity of 6800 N and a maximum speed of 22,000 rpm. These bearings serve as the primary anchoring elements, securing the shafts and the linked mechanical components within the enclosure. After the bearings come the final spacer and the pulley installation. The pulley has 25 teeth and is compatible with belts up to 15 mm wide. A dedicated slot establishes the key connection between the shaft and pulley. The coupling piece linking the motor's 12 mm shaft to the 6 mm gear motor represents the ultimate keyed element. Identical rotational speeds for both shafts result from the "pulley-belt" setup housed at the device's rear. This belt spans 525 mm and carries 105 teeth.

Given that shaft separation is less than 525 mm, engineers produced a PET-G tensioner fitted with ball bearings to maintain smooth "belt-pulley" performance. Parallel worm screws, positioned alongside the toothed wheel, ensure uninterrupted full rotation even if the 30-degree gap aligns with one screw. Under those conditions, the second screw alone temporarily sustains the turning action, visible on the left in **Figure 5**.

© 2025 The Author(s). | Published by Agro Intelligence Research Press

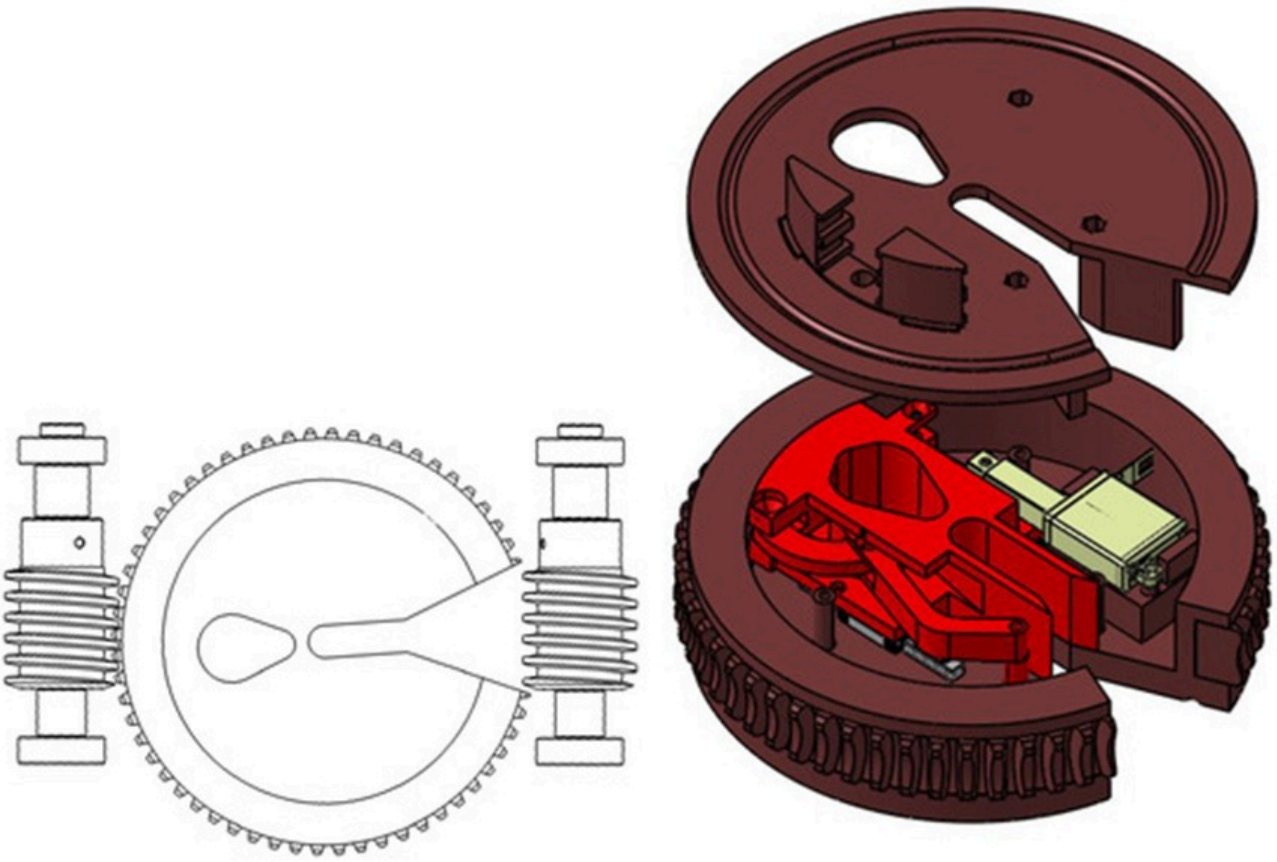

Figure 5. (Left): internal mechanism, and (right): wheeled tooth with internal guillotine system.

Five ball rollers per housing, each rated for a 2 N load, were added to promote easy wheel movement. They also create clearance between the wheel and the housing, minimizing contact friction on the PET-G surfaces.

Measuring 150 mm across, the toothed wheel features a 30-degree cutout that eases cable mounting and aligns the wheel's rotation axis with the cable's axis. This hollow wheel splits into a base container and a lid. Its outer surface bears teeth sized and counted according to worm screw specifications, yielding exactly 64 teeth **(visible on the right in Figure 5)**. A separate egg-shaped aperture, measuring up to 36×26 mm, aids the insertion of the diverter into the wheel.

A protruding feature on one wheel side **(Figure 6)** provides initial leverage against the diverter at the start of removal. Force calculations estimated roughly 58 N applied to the diverter, prompting gear-motor calibration that factored in the wheel-to-worm ratio and overall component friction.

© 2025 The Author(s). | Published by Agro Intelligence Research Press

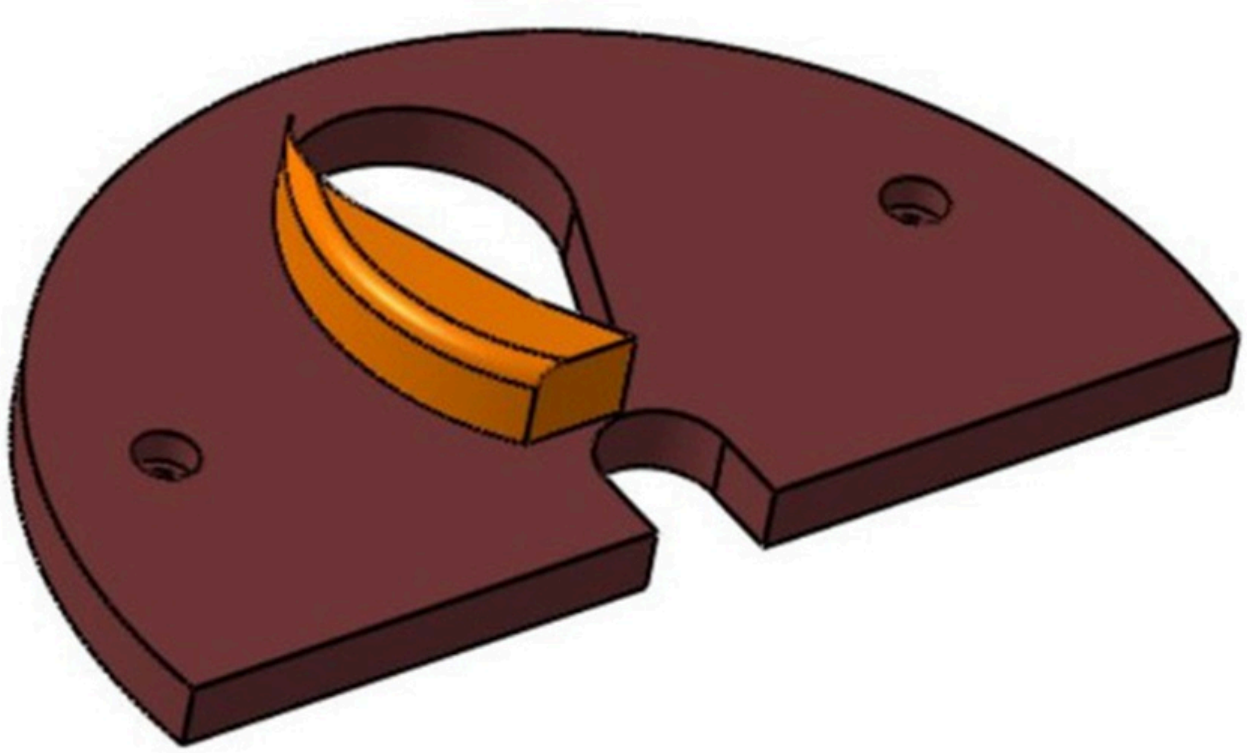

Figure 6. Protrusion.

A “guillotine” assembly sits inside the container, driven by a linear actuator along screw-fixed guides. Vertical displacement of this part clamps the diverter rigidly within the tool. Actuator retraction pulls the guillotine back, allowing left-side arms to swing inward via inertia and secure the item **(Figure 7)**. The design handles diverters up to 12 mm in diameter. Wheel protrusion provides continuous lever force on the diverter during toothed wheel rotation.

© 2025 The Author(s). | Published by Agro Intelligence Research Press

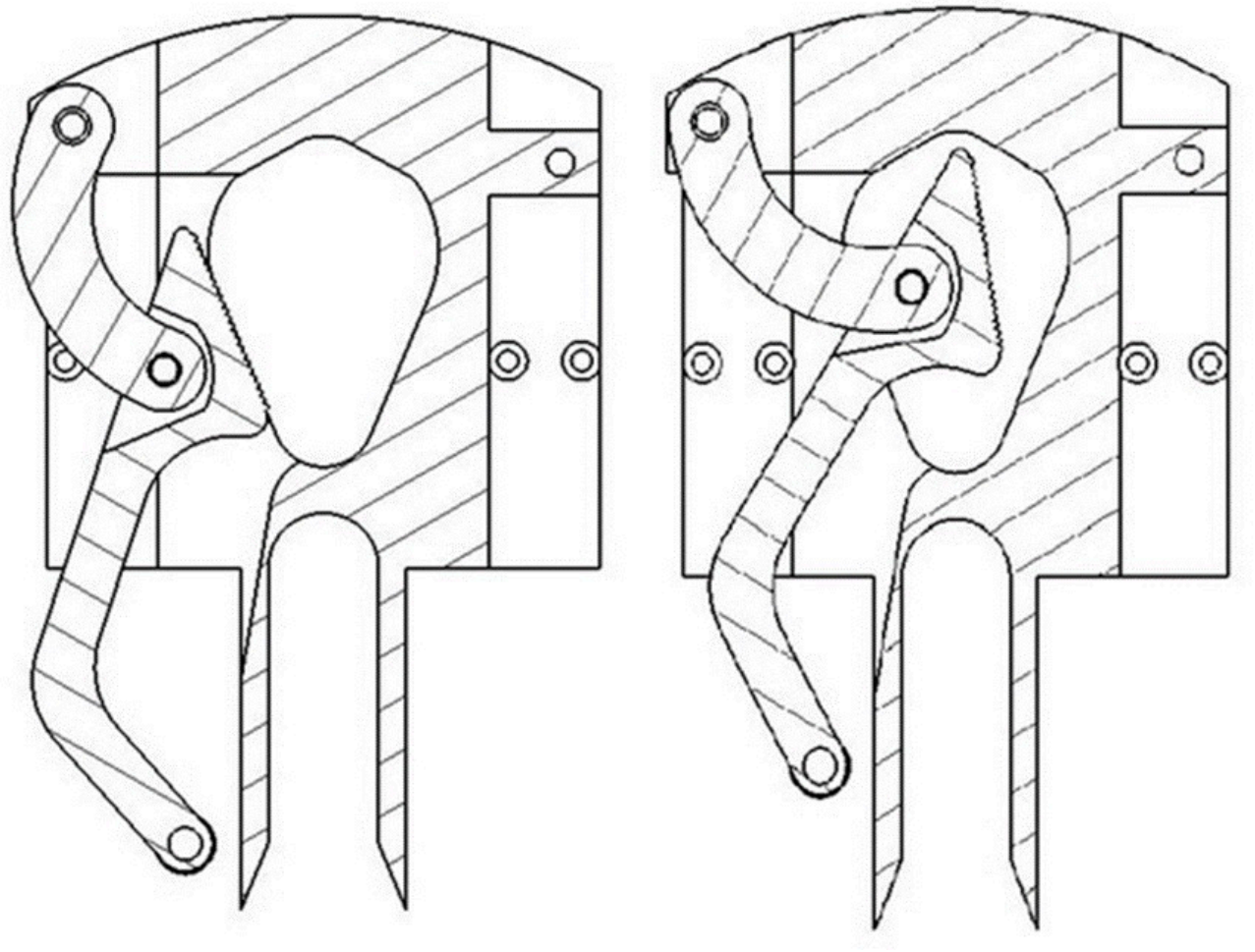

Figure 7. The guillotine mechanism acts like pincers to lock the diverter in place during the final phase of diverter removal.

Rear casing accommodates circuitry for device management. One protrusion facilitates attachment to the manipulator—a Kuka IIWA unit during trials **(Figure 8, left)** —though future versions can interface with drones. External mounting locations are available for the gear motor driver, with space on the opposite side reserved for the control microcontroller. This controller activates gripper functions according to external program signals. A serial bridge connection to the companion computer lets it receive on/off directives for stepper and motor drivers. Control software receives deeper coverage in Section 4.

© 2025 The Author(s). | Published by Agro Intelligence Research Press

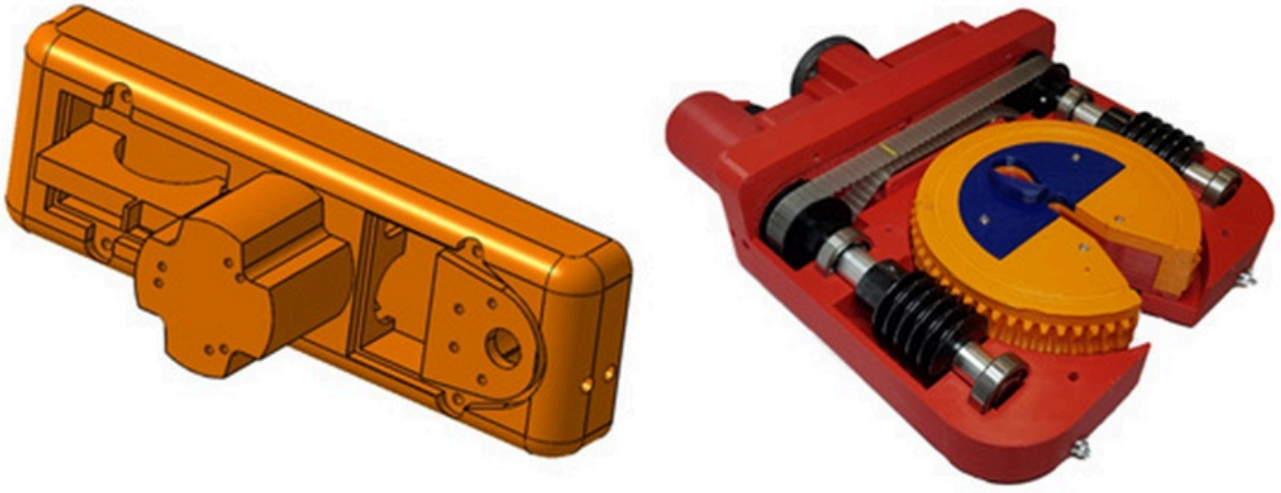

Figure 8. Left: the device's rear cover; right: its internal components.

The operation requires a 12-volt supply for the onboard microcontroller and mechanism drive. Standard four-cell LiPo batteries providing a nominal 14.8 V output (4 × 3.7 V) can power both UAV avionics and the gripper. The completed prototype visualization is on the right in **Figure 8**.

Development targeted diverters for cables no thicker than 11 mm, a constraint dictated chiefly by wheel size. This capacity nonetheless sufficed to validate prototype operations.

System Architecture

The overall system layout is illustrated in **Figure 9**.

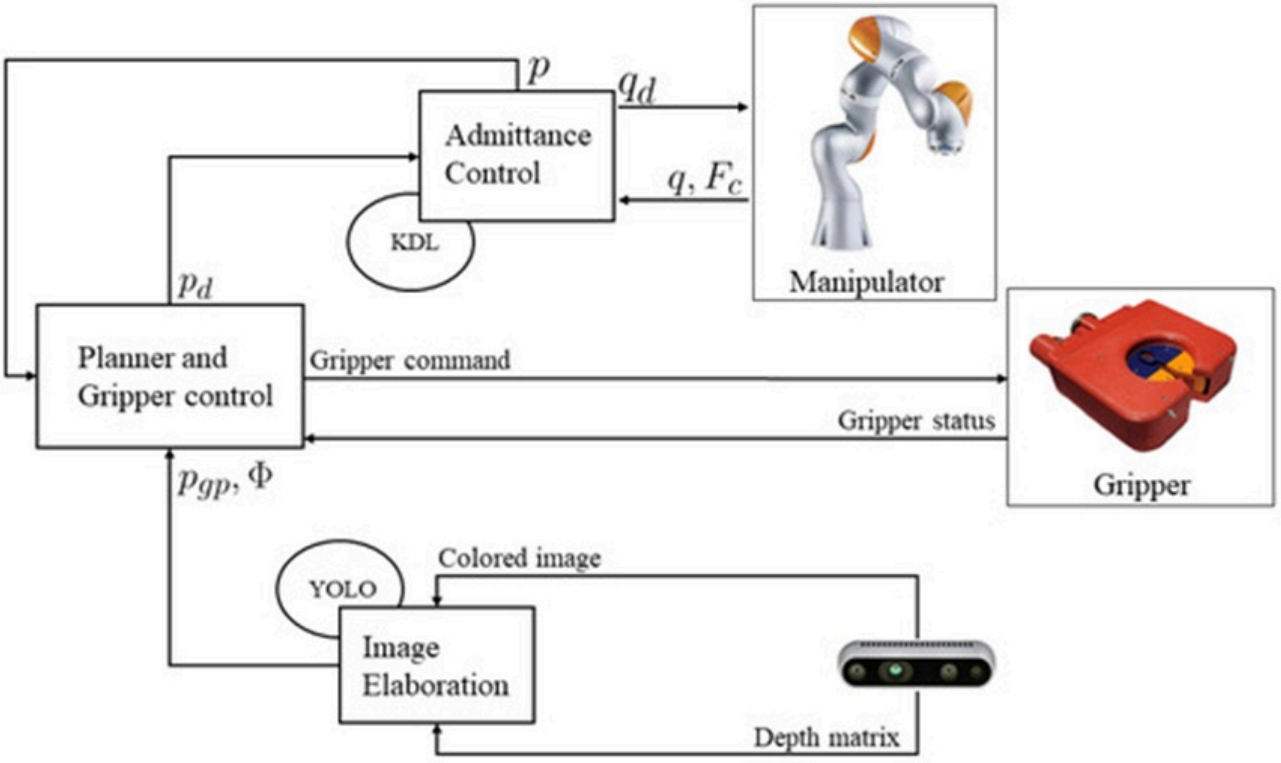

© 2025 The Author(s). | Published by Agro Intelligence Research Press

Figure 9. System architecture.

Inputs comprise color imagery and depth data matrices from the Intel 435d camera. These feed the Image Elaboration module, which takes color matrices and runs YOLO library routines to spot helical bird diverters. Neural networks inside YOLO enable swift, precise detection of object identity and placement. Relying on convolutional neural networks (CNNs), it achieves real-time results with a single forward pass, performing full-image prediction in a single operation. The module's depth matrix handling converts pixel data into 3D spatial coordinates. Training enabled YOLO to flag complete diverters for presence checks, plus two subsections labeled LD (Line Diverter) back and LD (Line Diverter) front to locate grasp spots. The trained model's output is displayed in the upper part of **Figure 10**.

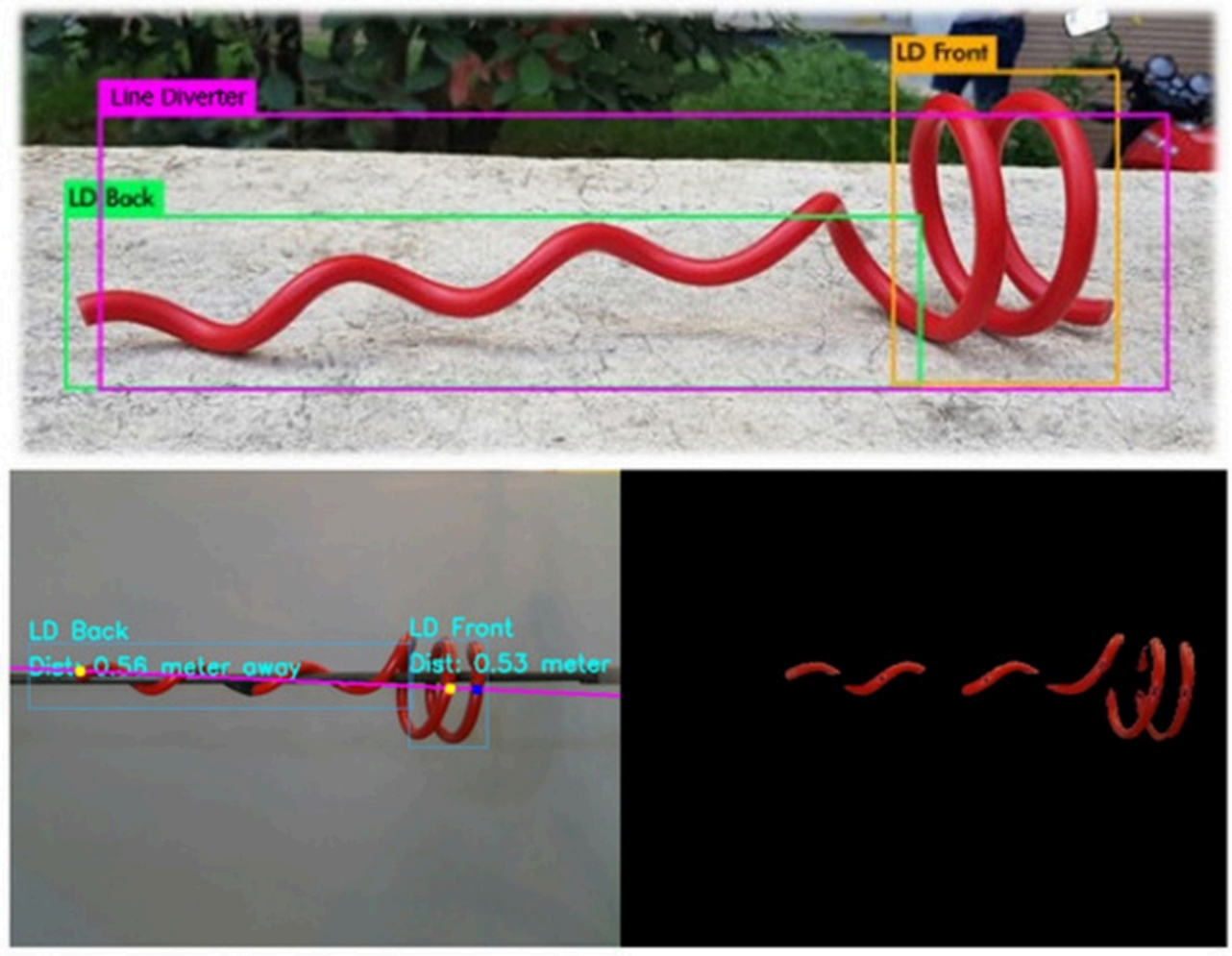

Figure 10. YOLO libraries in the detection of the helical diverter. Top: the raw output of the YOLO algorithm for a red helical diverter. Bottom: the image elaboration algorithm running as the output of the YOLO algorithm. In blue and yellow, possible grasping points.

For the studied removal scenario involving pre-installed diverters, YOLO provided additional details. Essential needs included grasp location and cable alignment. YOLO bounding data enabled image thresholding to isolate the diverter from surroundings **(bottom-right, Figure 10)**. Diverter pixels were then transformed into 3D points and interpolated into a pink line **(bottom-left, Figure 10)**. This line yielded two vital metrics: the far extremity opposite the large spirals marked the initial gripper placement (pgp, yellow dot far left in the bottom-left image), and line tilt across Euler angles for orientation to align the cable entry into the guillotine. Inter-spiral gaps on the LD front were also noted (yellow/blue dots, bottom-left image).

© 2025 The Author(s). | Published by Agro Intelligence Research Press

Image Elaboration therefore delivers the detected items and their characteristic points (grasp site and orientation) to the Planner and Gripper Control module. This directs manipulator and gripper actions to complete the task. Known 3D points relative to the camera are converted to manipulator base coordinates, enabling precise calculation of the device's contact location on the diverter. Coordinated manipulator-gripper movements execute the removal per Section 5 details. The serial interface handles communication between the gripper, the companion computer, and the internal microcontroller, exchanging guillotine commands and status updates.

Manipulator activation is mandatory for diverter handling. Testing used the seven-joint Kuka LBR iiwa arm with torque sensing on all axes. Java-based modular programming uses Kuka FRI libraries for direct joint positioning and solves kinematics on the companion computer. Task needs for guillotine-cable centering prompted the addition of force control to offset pose estimation inaccuracies, allowing physical contact to refine alignment. The Admittance Control module thus deploys Cartesian admittance control [33] based on end-effector forces. Dynamic force-motion linkage follows:

$$M_d\left(\ddot{X}_c - \ddot{X}_d\right) + D_d\left(\dot{X}_c - \dot{X}_d\right) + K_d\left(X_c - X_d\right) = F_c \quad (1)$$

Where Md, Dd, and $Kd \in \mathbb{R}3\times3$ denote positive definite diagonal matrices for virtual inertia, damping, and stiffness. Controller output produces compliant position $Xc \in \mathbb{R}3$ for the end effector from target $Xd \in \mathbb{R}3$. Inputs cover Planner-selected Cartesian Xd and measured end-effector force $Fc \in \mathbb{R}3$. Forward/inverse kinematics are used here as well, converting operational positions to joint targets and computing the current end-effector pose from joint data via the Kinematics and Dynamics Library (KDL).

Experiments

An autonomous removal trial evaluates prototype performance here, accompanied by a YOLO-based assessment of helical diverter detection.

The task overview sketch is shown in **Figure 11**, with the planned trajectory shown as a blue line and the diverter pose estimate positioned before the industrial arm.

© 2025 The Author(s). | Published by Agro Intelligence Research Press

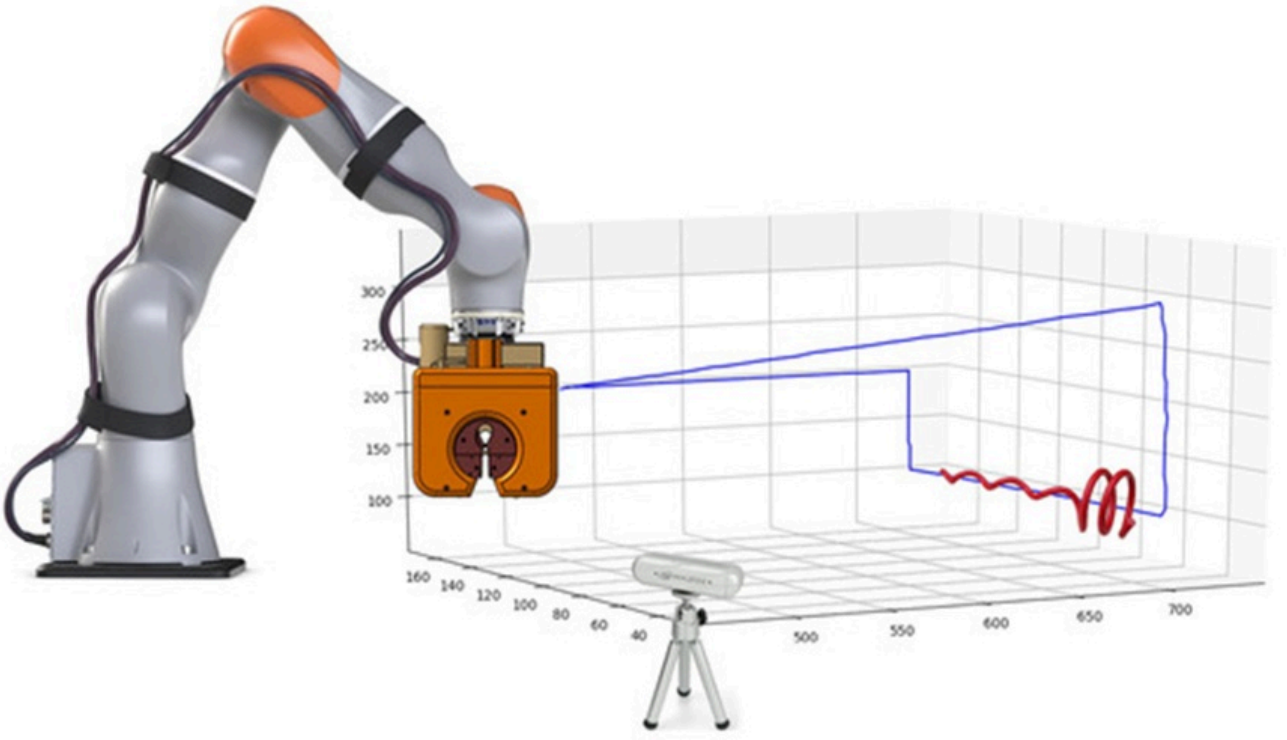

Figure 11. Mock-up.

Manipulator-gripper coordination drove the detailed sequence. Proper diverter handling requires dual rotations: clockwise for small-diameter initial spirals and counterclockwise for larger trailing ones during detachment **(Figure 2)**.

The steps shown in **Figure 12** structured the process. Post-detection, the approach targeted an overhead point above the grasp location using prior-image methods.

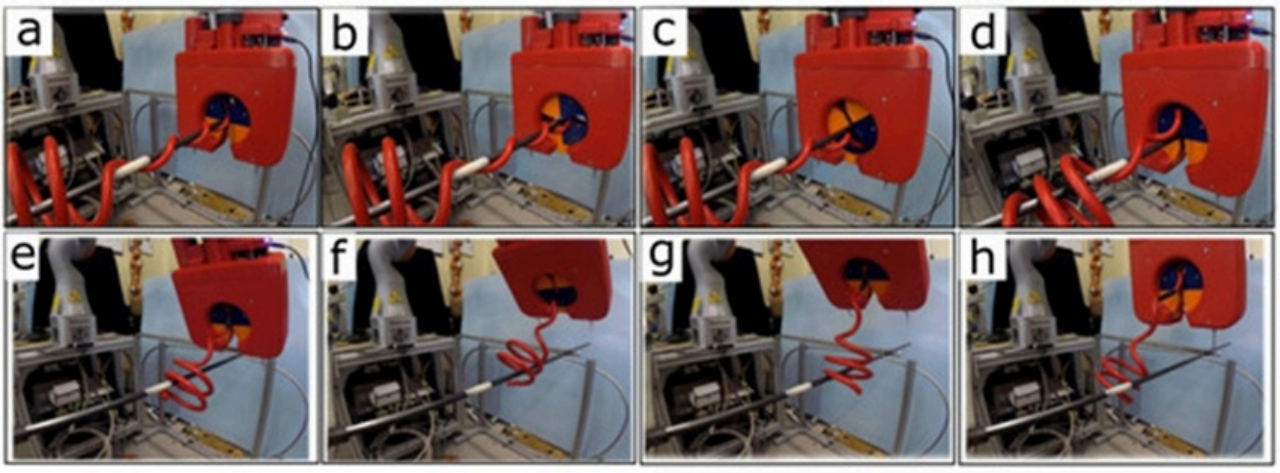

Figure 12. The different phases of the diverter removal process, from grasping to releasing. The full experiment can be seen at the following link https://youtu.be/-VVHq-wBBWA, accessed on 1 January 2023.

Vertical gripper placement preceded cable insertion through the tool opening **(Figure 12a)**. First gear wheel rotation then began **(Figure 12b)**. The linear manipulator advanced toward large spirals while the wheel spun. Admittance control maintained position stability until the sections were freed **(Figures 12c, 12d)**. Post-large-spiral clearance, end effector

© 2025 The Author(s). | Published by Agro Intelligence Research Press

angled relative to cable **(Figure 12e)** before guillotine closure. Counterclockwise wheel activation followed for the remaining attachment **(Figures 12f, 12g)**, ending with vertical withdrawal **(Figure 12h)**.

Waypoints from the depth sensor diverter pose generated trapezoidal paths. Admittance tuning prevented premature forcing until cable release progressed.

Figure 13 captures the pilot helical diverter removal case. Logged data included end-effector Cartesian position/orientation **(Figures 13 and 14)** and gripper forces **(Figure 15)**. Cable alignment was parallel to the robot's x-axis, so the initial motion reached the line **(first graph, Figure 13)**. Y-motion graph tracked along-cable progress. **Figure 14** revealed a single orientation shift in the final extraction, with yaw remaining unchanged due to task alignment.

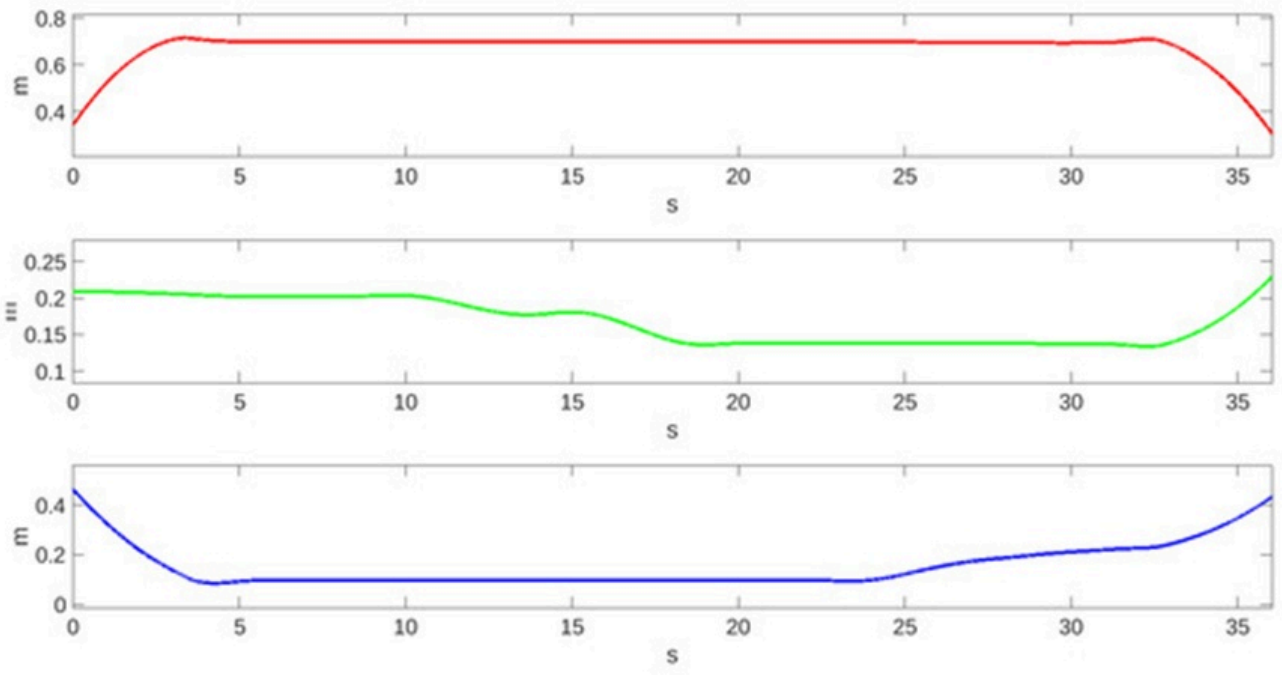

Figure 13. Time series of the position of the end effector during the task. Red: x; green: y; blue: z.

© 2025 The Author(s). | Published by Agro Intelligence Research Press

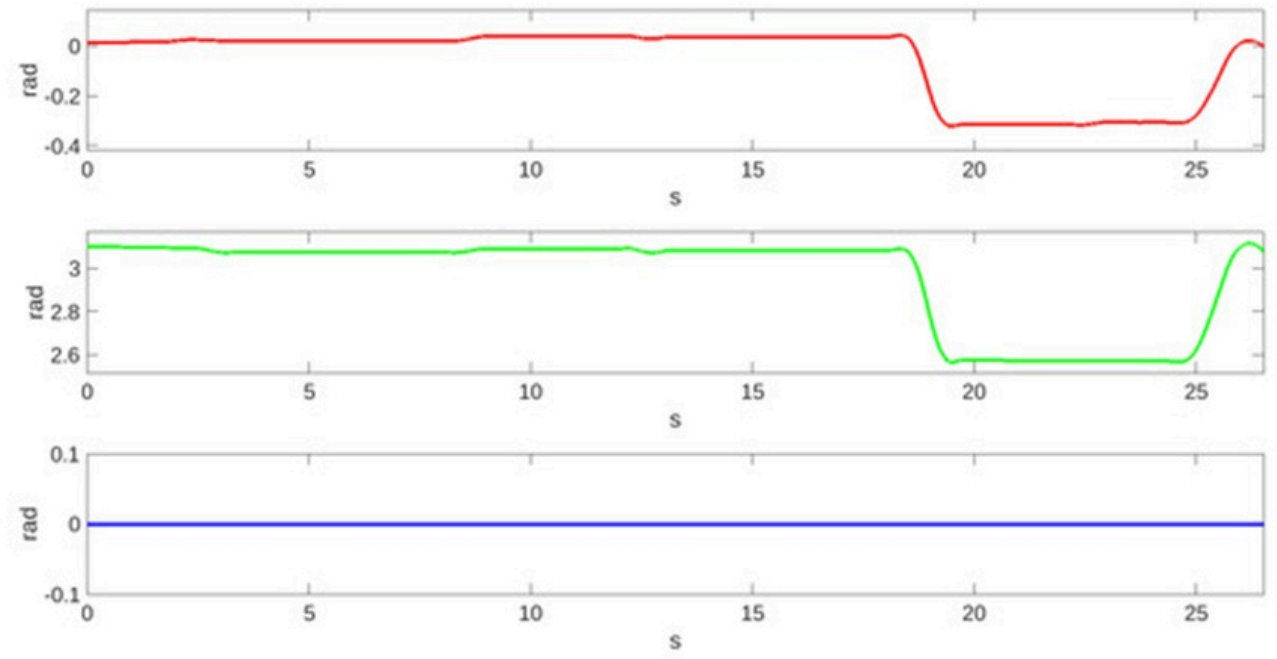

Figure 14. Time series of the orientation of the end effector during the task. Red: roll; green: pitch; blue: yaw.

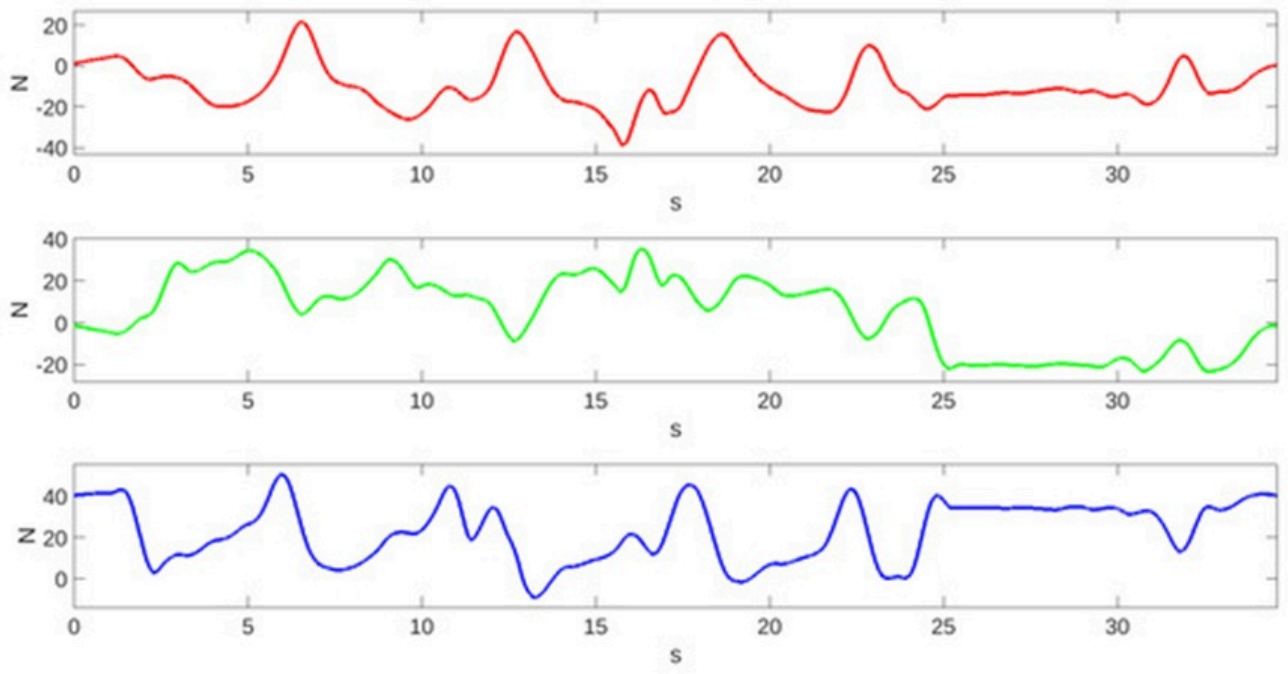

Figure 15. Time series of the estimated end-effector force during the task. Red: x; green: y; blue: z.

Removal forces on the end effector **(Figure 15)** showed prominent peaks at cable contacts and during wide-spiral disengagement.

To enable reliable identification of the helical diverter, the YOLOv4 algorithm was appropriately trained. Multiple photographs captured under varying dimensions and illumination settings were utilized. Specifically, 120 pictures were

© 2025 The Author(s). | Published by Agro Intelligence Research Press

used for system training, with the Google Colab [34] hardware accelerator employed. Each image had labels applied to the diverter and its subsections: the full diverter, LD front, and LD back.

The trained network underwent evaluation on a dedicated test set of 400 images. Here, 80% of the images featured the diverter on the ground or attached to power lines, while the remaining 20% depicted power line cables without any bird diverters. Performance of the recognition setup was measured via accuracy percentage, αa, derived from this equation:

$$\alpha_a = \frac{T_P + T_N}{T_P + T_N + F_P + F_N} \quad (2)$$

Where TP denotes true positive, TN true negative, FP false positive, and FN false negative. These metrics reflected the percentage of instances in which the detector correctly identified the diverter in images. Outcomes are presented in **Table 1**, showing accuracy percentages for all identifiable elements using the YOLO library.

Table 1. Object detection performed with YOLO version 4 evaluation.

Object	FN	FP	TN	TP	Accuracy
Diverter	0.18%	0.06%	0.81%	0.93%	0.87%
LD Back	0.06%	0.09%	0.93%	0.90%	0.92%
LD Front	0.18%	0.12%	0.81%	0.87%	0.84%

Findings from **Table 1** confirm that the vision setup successfully located both the complete diverter and its components. This capability supplied the control system with data on diverter alignment, specifically enabling grasp point determination.

Conclusion

The present study introduced an innovative robotic gripper intended for handling helical bird diverters. Such equipment reduces impacts between birds and power lines, thereby limiting fatalities among flying creatures. Given their intricate forms, fitting and detaching these items proves challenging and typically falls to human workers facing risky, high-stakes situations. Shifting this activity to an aerial manipulator marks a significant advance toward protecting operator wellbeing. Accordingly, the examination covered diverter configuration and associated handling techniques. A mechanical gripper blueprint for helical bird diverter detachment was developed, paired with an automated detection framework that locates diverters on lines and maps their spatial coordinates. Integration with an industrial manipulator was performed to support initial validation. The examined scenario validated the gripper's practical value.

Regarding constraints in this research, the analyzed scenario addressed the detachment of the helical component from the cable. It omitted broader dynamic influences present in actual operations, particularly manipulation impacts on a mobile platform. Nonetheless, current UAV capabilities support the creation of aerial platforms with substantial carrying capacity and adjustable rotors for environmental engagement and the application of considerable interaction forces [35, 36]. Moreover, tailored low-level controls for flying units can mitigate external interference, such as wind, during task execution [37, 38].

© 2025 The Author(s). | Published by Agro Intelligence Research Press

Subsequent efforts should refine the gripper construction to lower its overall mass. Concurrently, trials must be conducted in authentic field conditions using an aerial manipulator.

Acknowledgements

None

Conflict of interest

None

Financial support

The research leading to these results has been supported by the AERIAL-CORE project (Horizon 2020 Grant Agreement No. 871479). The authors are solely responsible for its content.

Ethics statement

None

Received: 18 Dec 2023 Revised: 22 Feb 2024 Accepted: 10 Mar 2024
Published online: 25 November 2025

Rights and permissions

Open Access The author(s) retain copyright. This article is licensed under the Creative Commons Attribution-NonCommercial-ShareAlike 4.0 International License. It may be shared and adapted for non-commercial purposes with appropriate attribution, an indication of changes, and distribution of adaptations under the same license. Third-party material may be subject to separate terms identified in its credit line. View the license at https://creativecommons.org/licenses/by-nc-sa/4.0/.

References

1. Ferrer M. Birds and Power Lines: From Conflict to Solution; ENDESA SA and Fundación MIGRES: Sevilla, Spain, 2020.

2. Manville AM. The ABCs of avoiding bird collisions at communication towers: The next steps. In Proceedings of the Workshop on Avian Interactions with Utility and Communication Structures, Charleston, SC, USA, 1999; Electric Power Research Institute: Palo Alto, CA, USA, 1999. p. 85–103.

3. Manville AM. Towers, turbines, power lines, and buildings–steps being taken by the US Fish and Wildlife Service to avoid or minimize take of migratory birds at these structures. In Proceedings of the Fourth International Partners in Flight Conference: Tundra to Tropics, McAllen, TX, USA, 2008; 262272.

4. Jenkins AR, Smallie JJ, Diamond M. Avian collisions with power lines: A global review of causes and mitigation with a South African perspective. Bird Conserv Int. 2010;20:263–78.

5. Bevanger K. Estimating Bird Mortality Caused by Collision with Power Lines and Electrocution, a Review of Methodology.–S. 29-56 i Ferrer M and Janss, GFE (Red.), Birds and Power Lines. Collision, Electrocution and Breeding; Quercus: Madrid, Spain, 1999.

6. Ferrer M, Morandini V, Baumbusch R, Muriel R, De Lucas M, Calabuig C. Efficacy of different types of “bird flight diverter” in reducing bird mortality due to collision with transmission power lines. Glob Ecol Conserv. 2020;23:e01130.

7. Ruggiero F, Lippiello V, Ollero A. Aerial manipulation: A literature review. IEEE Robot Autom Lett. 2018;3:1957–64.

8. Cacace J, Fontanelli GA, Lippiello V. A novel hybrid aerial-ground manipulator for pipeline inspection tasks. In: Proceedings of the 2021 Aerial Robotic Systems Physically Interacting with the Environment (AIRPHARO), Biograd na Moru, Croatia, 2021. p. 1–6.

9. Ollero A, Heredia G, Franchi A, Antonelli G, Kondak K, Sanfeliu A, et al. The AEROARMS project: Aerial robots with advanced manipulation capabilities for inspection and maintenance. IEEE Robot Autom Mag. 2018;25:12–23.

10. Lippiello V, Cacace J. Robust visual localization of a UAV over a pipe-rack based on the Lie Group SE(3). IEEE Robot Autom Lett. 2022;7:295–302.

11. Trujillo MA, Martínez-de Dios JR, Martín C, Viguria A, Ollero A. Novel aerial manipulator for accurate and robust industrial NDT contact inspection: A new tool for the oil and gas inspection industry. Sensors. 2019;19:1305.

12. Ikeda T, Yasui S, Fujihara M, Ohara K, Ashizawa S, Ichikawa A, et al. Wall contact by octo-rotor UAV with one DoF manipulator for bridge inspection. In: Proceedings of the 2017 IEEE/RSJ International Conference on Intelligent Robots and Systems (IROS), Vancouver, BC, Canada; 2017. p. 5122–7.

13. Suarez A, Real F, Vega VM, Heredia G, Rodriguez-Castaño A, Ollero A. Compliant bimanual aerial manipulation: Standard and long reach configurations. IEEE Access. 2020;8:88844–65.

14. Hamaza S, Georgilas I, Fernandez M, Sanchez P, Richardson T, Heredia G, et al. Sensor installation and retrieval operations using an unmanned aerial manipulator. IEEE Robot Autom Lett. 2019;4:2793–800.

15. Orsag M, Korpela C, Bogdan S, Oh P. Valve turning using a dual-arm aerial manipulator. In: Proceedings of the 2014 International Conference on Unmanned Aircraft Systems (ICUAS), Orlando, FL; 2014. p. 836–41.

16. Shimahara S, Leewiwatwong S, Ladig R, Shimonomura K. Aerial torsional manipulation employing multi-rotor flying robot. In: Proceedings of the 2016 IEEE/RSJ International Conference on Intelligent Robots and Systems (IROS), Daejeon, Republic of Korea; 2016. p. 1595–600.

17. Meng J, Buzzatto J, Liu Y, Liarokapis M. On aerial robots with grasping and perching capabilities: A comprehensive review. Front Robot AI. 2022;8:739173.

18. Kondak K, Huber F, Schwarzbach M, Laiacker M, Sommer D, Bejar M, et al. Aerial manipulation robot composed of an autonomous helicopter and a 7 degrees of freedom industrial manipulator. In: Proceedings of the 2014 IEEE International Conference on Robotics and Automation (ICRA), Hong Kong, China; 2014. p. 2107–12.

19. Mirallès F, Hamelin P, Lambert G, Lavoie S, Pouliot N, Montfrond M, et al. LineDrone technology: Landing an unmanned aerial vehicle on a power line. In: Proceedings of the 2018 IEEE International Conference on Robotics and Automation (ICRA), Brisbane, Australia; 2018. p. 6545–52.

20. Iversen N, Kramberger A, Schofield OB, Ebeid E. Pneumatic-mechanical systems in UAVs: Autonomous power line sensor unit deployment. In: Proceedings of the 2021 IEEE International Conference on Robotics and Automation (ICRA), Xi’an, China; 2021. p. 548–54.

© 2025 The Author(s). | Published by Agro Intelligence Research Press

21. Suarez A, Romero H, Salmoral R, Acosta JA, Zambrano J, Ollero A. Experimental evaluation of aerial manipulation robot for the installation of clip type bird diverters: Outdoor flight tests. In: Proceedings of the 2021 Aerial Robotic Systems Physically Interacting with the Environment (AIRPHARO), Biograd na Moru, Croatia; 2021. p. 1–7.

22. Armengol I, Suarez A, Heredia G, Ollero A. Design, integration and testing of compliant gripper for the installation of helical bird diverters on power lines. In: Proceedings of the 2021 Aerial Robotic Systems Physically Interacting with the Environment (AIRPHARO), Biograd na Moru, Croatia; 2021.p. 1–8.

23. Erlingsson BF, Hreimsson I, Pálsson PI, Hjálmarsson SJ, Foley JT. Axiomatic design of a linear motion robotic claw with interchangeable grippers. Procedia CIRP. 2016;53:213–8.

24. Xu Z, Kumar V, Todorov E. A low-cost and modular, 20-DOF anthropomorphic robotic hand: Design, actuation and modeling. In: Proceedings of the 2013 13th IEEE-RAS International Conference on Humanoid Robots (Humanoids), Atlanta, GA, USA; 2013. p. 368–75.

25. Xu Z, Todorov E. Design of a highly biomimetic anthropomorphic robotic hand towards artificial limb regeneration. In: Proceedings of the 2016 IEEE International Conference on Robotics and Automation (ICRA), Stockholm, Sweden; 2016. p. 3485–92.

26. Dhanawade MDA, Sabnis MNV. A review: State of the art of robotic grippers. Int Res J Eng Technol. 2018;5:371–5.

27. Shintake J, Cacucciolo V, Floreano D, Shea H. Soft robotic grippers. Adv Mater. 2018;30:1707035.

28. LiCAS. Licas Robotic Arms. https://licas-robotic-arms.com/ (accessed on 1 January 2023).

29. Suarez A, Sanchez-Cuevas PJ, Heredia G, Ollero A. Aerial physical interaction in grabbing conditions with lightweight and compliant dual arms. Appl Sci. 2020;10:8927.

30. Cuniato E, Cacace J, Selvaggio M, Ruggiero F, Lippiello V. A hardware-in-the-loop simulator for physical human-aerial manipulator cooperation. In: Proceedings of the 2021 20th International Conference on Advanced Robotics (ICAR), Ljubljana, Slovenia; 2021.p. 830–5.

31. Jiang P, Ergu D, Liu F, Cai Y, Ma B. A review of YOLO algorithm developments. Procedia Comput Sci. 2022;199:1066–73.

32. Dewi C, Chen RC, Liu YT, Jiang X, Hartomo KD. YOLO v4 for advanced traffic sign recognition with synthetic training data generated by various GAN. IEEE Access. 2021;9:97228–42.

33. Hogan N. Impedance control: An approach to manipulation. In: Proceedings of the 1984 American Control Conference, San Diego, CA, USA; 1984. p. 304–13.

34. Paper D. Build your first neural network with Google Colab. In: TensorFlow 2.x in the Colaboratory Cloud: An Introduction to Deep Learning on Google's Cloud Service; Apress: Berkeley, CA, USA; 2021. p. 25–45.

35. Ollero A, Tognon M, Suarez A, Lee D, Franchi A. Past, present, and future of aerial robotic manipulators. IEEE Trans Robot. 2022;38:626–45.

36. Heredia G, Jimenez-Cano A, Sanchez I, Llorente D, Vega V, Braga J, et al. Control of a multirotor outdoor aerial manipulator. In: Proceedings of the 2014 IEEE/RSJ International Conference on Intelligent Robots and Systems (IROS), Chicago, IL, USA; 2014. p. 3417–22.

37. Ruggiero F, Cacace J, Sadeghian H, Lippiello V. Passivity-based control of VToL UAVs with a momentum-based estimator of external wrench and unmodeled dynamics. Robot Auton Syst. 2015;72:139–51.

© 2025 The Author(s). | Published by Agro Intelligence Research Press

38. Morlando V, Ruggiero F. Disturbance rejection for legged robots through a hybrid observer. In: Proceedings of the 2022 30th Mediterranean Conference on Control and Automation (MED), Athens, Greece, 2022; pp. 743–8.

© 2025 The Author(s). | Published by Agro Intelligence Research Press